JOURNAL OF BACTERIOLOGY, Feb. 1974, p. 844-857

Vol. 117, No. 2
Printed in U.S.A.

Plain and Complex Flagella of *Pseudomonas rhodos*: Analysis of Fine Structure and Composition

RÜDIGER SCHMITT, IVAN RASKA,[1] AND FRANK MAYER[2]

Institut für Mikrobiologie, Universität Erlangen-Nürnberg, 852 Erlangen, Friedrichstrasse 33, Germany, and Institut de Biologie Moléculaire, Université de Genève, Switzerland

Received for publication 17 October 1973

Cells of *Pseudomonas rhodos* 9-6 produce two morphologically distinct flagella termed plain and complex, respectively. Fine structure analyses by electron microscopy and optical diffraction showed that plain flagellar filaments are cylinders of 13-nm diameter composed of globular subunits like normal bacterial flagella. The structure comprises nine large-scale helical rows of subunits intersecting four small-scale helices of pitch angle 25°. Complex filaments have a conspicuous helical sheath, 18-nm wide, of three close-fitting helical bands, each about 4.7-nm wide, separated by axial intervals, 4.7 nm wide, running at an angle of 27°. The internal core has similar but not identical substructure to plain filaments. Unlike plain flagella, the complex species is fragile and does not aggregate in bundles. Mutants bearing only one of two types of flagellum were isolated. Cells with plain flagella showed normal translational motion, and cells with complex flagella showed rapid spinning. Isolated plain flagella consist of a 37,000-dalton subunit separable into two isoproteins. Complex filaments consist of a 55,000-dalton protein; a second 43,000-dalton protein was assigned to complex flagellar hooks. The results indicate that plain and complex flagella are entirely different in structure and composition and that the complex type represents a novel flagellar species. Its possible mode of action is discussed.

Bacterial flagella consist of three parts: a basal region attached to the plasma membrane, a hook-like structure terminating at or partially protruding from the cell surface, and a long helical filament external to the cell (1, 23). The composition of flagellar filaments of different bacteria have been studied extensively (2, 8). The flagellin subunits (molecular weight 40,000) are arranged helically into a cylindrical structure which itself is coiled into a helix. This is seen as a sinusoidal wave in electron micrographs. The superfolding of the filament leads to a typical subunit arrangement into small-scale and large-scale helices as revealed by fine structure analyses (4, 16, 19).

The flagella of *Pseudomonas rhodos* 9-6, a soil bacterium isolated and first described by Heumann (7), exhibit unusual features. Previous studies (14, 15) have indicated two types of flagella. One type resembles the flagella of other bacteria. The second type shows an unusual line with periodic undulations due to a flagellar sheath consisting of close-fitting helically wound bands (16). The intervals between neighboring bands disclose longitudinal lines which have been attributed to a filamentous core inside the helical superstructure by Lowy and Hanson (15). They assumed that there was a single type of filament which was either naked or sheathed. The present investigation indicates that there are two distinct types of filament structures, resulting in two quite different types of flagella. To account for their distinctive morphology, we have introduced the terms plain and complex for sheathless and sheathed flagella, respectively. The hooks of plain and complex flagella are characteristically different from each other. Their structure has been analyzed and will be described in a subsequent article (Raska, Mayer, and Schmitt; in preparation).

[1] Present address: Czechoslovak Academy of Sciences, Prague 2, Albertov 4, CSSR.

[2] Present address: Institut für Mikrobiologie, Universität Göttingen, 34 Göttingen, Germany.

MATERIALS AND METHODS

Media. The composition of the minimal medium (MM) was as follows (per liter): KH_2PO_4, 2 g; K_2HPO_4, 7 g; $(NH_4)_2SO_4$, 1 g; $MgSO_4 \cdot 7H_2O$, 0.1 g; sodium citrate, 0.3 g; cobalamin, 0.2 g; biotin, 0.025 mg; riboflavine, 0.025 mg; glucose, 5 g; nutrient broth (Difco), 0.1 g; and agar, 18 g. The complete medium (CM) employed was nutrient broth (Difco), 8 g/liter,

solidified with 16 g of agar per liter. The temperature of incubation throughout was 30 C.

Bacterial strains. Wild-type *P. rhodos* 9-6 was obtained from the collection of W. Heumann, University of Erlangen (7). Two mutant strains were used, D8, having only plain flagella, and B9, having only complex flagella.

Mutagenesis. Mutagenesis of strain 9-6 was carried out in broth containing 100 μg of *N*-methyl-*N'*-nitro-*N*-nitroso guanidine (NTG) per ml for 5 h at 30 C. Mutants having only one of two types of flagella were identified by direct electron microscope screening.

Isolation and purification of flagella. Flagellar preparations were obtained as follows. A single colony was subcultured twice serially on MM to give sufficient cells to inoculate 300 CM plates. The resulting lawns were harvested and washed once with 0.85% saline. Suspensions of approximately 10^{10} cells per ml with added glass beads (2 mm diameter) were shaken vigorously for 1 min on a reciprocal shaker (1,400 strokes per min) and sedimented at 10,000 $\times$ *g* for 5 min. Sediments were suspended in saline, and the above procedure was repeated. Because the complex flagella are more fragile, the glass beads were omitted for their preparation. The pooled supernatants containing flagella and cellular fragments were purified by two series of differential centrifugations, first at 15,000 $\times$ *g* for 10 min and 100,000 $\times$ *g* for 8 h and second at 1,500 $\times$ *g* for 10 min and 80,000 $\times$ *g* for 1 h. During the last high-speed sedimentation, flagella were concentrated on a 60% sucrose shelf in a swing-out rotor. The sediment contained more than 90% flagellar material as determined by electron microscopy and sodium dodecyl sulfate (SDS) gel electrophoresis.

Degradation of complex flagella. To a 2-ml sample of complex flagella (2 to 4 mg of protein per ml), solid urea was added to give a final concentration of 6 M. The mixture was kept at 25 C. Samples of 0.2 ml were withdrawn at intervals and immediately diluted into 4 ml of ice-cold distilled water. The partially degraded flagella were sedimented at 100,000 $\times$ *g* for 60 min. The sediments were analyzed both by electron microscopy and SDS gel electrophoresis. For enzymatic degradation, the flagellar suspension was incubated at 37 C with the enzyme (100 μg/ml final concentration) and sampled as described above. The enzymes employed were Pronase, trypsin, chymotrypsin, hyaluronidase, glucuronidase, and lipase from *Aspergillus* (all Serva, Heidelberg).

Acrylamide gel electrophoresis. Crude and purified preparations of flagella containing 2 to 4 mg of protein per ml (13) were preincubated with 1% SDS and 1% 2-mercaptoethanol and analyzed by continuous SDS gel electrophoresis using 7.5 or 10% acrylamide by the method of Shapiro et al. (20). The molecular weights of standard markers (serum albumin, ovalbumin S, pepsin, and chymotrypsinogen from Serva, Heidelberg) were plotted against their relative electrophoretic mobilities (28). From this plot the molecular weight of each unknown protein was determined (20, 28). Electrophoreses were performed at a constant voltage of 6 V/cm for 5 to 6 h. Alternatively, flagella were dissociated in 8 M urea and analyzed by electrophoresis in a 10% discontinuous acrylamide gel (pH 4.5) containing 8 M urea (25). A constant current of 3.5 mA per tube was employed; the migration at 4 C lasted 24 h. Protein bands were stained (6) with 0.25% Coomassie brilliant blue R 250 (Serva, Heidelberg). Staining of glycoproteins with Alcian blue (Serva, Heidelberg) was performed by the method of Wardi et al. (27). The intensity of stained bands was determined by densitometric scanning with a Gilford 2400 spectrophotometer at 600 nm.

Phase-contrast microscopy. The motility of exponentially growing cells was examined with a Zeiss microscope.

Electron microscopy. Negatively stained samples were prepared by the procedure of Valentine et al. (26) with 2% potassium phosphotungstate (pH 7.0), 2% uranyl acetate (pH 4.8), or uranyl formate (pH 4.8), respectively. Microscope magnifications were tested by employing either a replica of an optical grating or a shadowed preparation of Latex spheres. The microscopes employed were a JEM 7A (JEOL, Japan Electron Optics Laboratory Co., Ltd.) or a 6 B (AEI Scientific Apparatus Ltd., Manchester, England).

Optical diffraction and filtering. Optical diffractions of electron micrographs were taken with the diffractometer, as described by Yanagida et al. (29), and a commercial diffractometer (Polaron Instruments LTD, London). Copies of electron micrographs on film (magnification: $\times$25,000 to $\times$160,000) were employed for optical diffraction (29). Diffraction patterns were evaluated by selecting the main reflections which define the reciprocal lattice (10). Filtering experiments were performed by the method of Klug and De Rosier (11). The original diffraction negative, after punching of the appropriate reflections, was stained with a solution of 1% amido black B (Serva, Heidelberg) in 7.5% acetic acid and then used as an optical filter. Each aperture of the filter mask was made large enough to transmit all the diffracted beam at each reciprocal lattice point. In case of one-sided reconstructions, the origin was covered with a copper screen (fine mesh) to eliminate about half of the intensity of the direct beam.

RESULTS

Characteristics of P. rhodos 9-6 and its mutants. Exponentially growing wild-type cells from a single clone showed two types of motion, namely the normal translational type of motion and also a rapid spinning or tumbling motion clearly different from the former. Within the population, individual cells showed only one or the other type of motion, implying that these individuals carry one or the other flagellar species. Both mutant types were motile. Cells with plain flagella (strain D8) showed translational motion, whereas those with complex flagella (strain B9) showed the spinning motion. These mutants were isolated from a NTG-treated stock of the wild-type strain 9-6. Out of 200 colonies screened by electron microscopy,

five mutants were obtained, two producing only plain flagella and three only complex flagella. All mutants were stable with respect to their flagellar markers and did not revert either spontaneously or after mutagenic treatment with NTG or ultraviolet light.

Gross morphology of the flagella. Electron micrographs of negatively stained flagellar preparations of *P. rhodos* 9-6 show two distinct filamentous structures occurring in about equal proportions (Fig. 1). Plain filaments exhibit the typical sinusoidal curvature, and side-by-side aggregates can be observed frequently. Measurements of the width of a single flagellum gave an average value of 13 nm. Complex flagella distinguishable by the prominent pattern of helical bands generally appear as straight or slightly curved filaments and show a pronounced tendency to break. Examination of many such breaks never revealed the naked core as would be expected if the structures of core and sheath were less intimately connected. In agreement with reported data (15, 17), the width of complex filaments was found to range between 18 and 19 nm. Hooks of both flagellar species can be observed frequently when flagella become detached from the bacterium (Fig. 1). The cone-shaped hooks of plain flagella differ characteristically from those of the complex type, which appear as long cylinders of distinct fine structure.

Fine structure of the plain filament. Figure 2a shows a high-resolution electron micrograph of a plain flagellum. Reflections in the diffractogram (Fig. 2b) are located near the equator at 3.7 nm^{-1}. In addition, strong reflections appear on layer lines at spacings of 4.5 and 2.25 nm^{-1}, respectively, indicating a helical arrangement of subunits in the flagellar structure (10). This arrangement becomes clear in the one-sided optical reconstruction (Fig. 2c) obtained by employing the principal maxima (near-equatorial at 3.7 nm^{-1} spacing and reflections on layer lines of 4.5 nm^{-1} spacing) for filtering (11). The reconstructed image reveals a maximum of five longitudinal rows of subunits of pitch angle greater than 85° intersecting a set of helical grooves of pitch angle approximately 25°. The partial deformation of the near-hexagonal surface lattice may be caused by the flattening of the original structure during preparation. This is supported by the absence of well-developed subsidiary maxima on the principal layer lines in the diffractogram (Fig. 2b), which would be expected for a well-conserved helical lattice (18, 19) and also by a measurement of the particle width in Fig. 2a, that yields an average value of 21 nm as contrasted to a reported flagellar diameter of 13 nm (15). The latter value also has been obtained by examination of a bundle of plain flagella in which the filaments lie side by side. The approximate value for the lateral separation of longitudinal lines on the flagellar surface which can be calculated from the equatorial spacing of 3.7 nm^{-1} (Fig. 2b) is about 4.5 nm (4). By relating this value to the circumference of the flagellar cylinder of 13-nm diameter, the number of longitudinal rows is 9. From this it appears that the general structure of the plain flagellum of *P. rhodos* 9-6 agrees broadly with those reported for other bacterial flagella (4, 16, 19).

Fine structure of the complex filament. The morphology of complex flagella is dominated by the prominent undulations of the helical sheath (Fig. 3a). Less obvious are several near-axial lines believed to originate from the internal core (14, 15). The diffraction pattern of a complex filament shown in Fig. 3b is due mainly to the sheath structure. The principal maxima on layer lines of 9.4 nm^{-1} spacing are determined by the axial separation of neighboring helical chains. Reflections along these layer lines do not show complete meridional symmetry owing to a different degree of preservation and staining on the two sides of the flagellar particles in Fig. 3a (18). However, the presence of subsidiary maxima further from the meridian indicates no extensive flattening of the helical structure. For a cylindrical structure, calculations based on the radial distances of the principal maxima yield a diffracting radius of 8.3 to 10 nm (4) which is consistent with the measured flagellar diameter of 18 to 19 nm. Figure 3c shows the diffraction pattern with a reciprocal lattice superimposed. A one-sided reconstruction of the sheath (Fig. 3d) was obtained by using maxima located on the reciprocal lattice for optical filtering and by omitting the equatorial reflections at 3.6 nm^{-1} spacing, which obviously arise from a lower diffracting radius. The corresponding surface lattice can be described by a unit cell of a = 9.4 nm (axial distance of helical chains) and b = 5.3 nm (lateral distance of subunits in one chain) for a diffracting radius of 8.5 nm; the angular pitch is approximately 27°. It is assumed that reflections from different helical directions originate from approximately the same diffracting radius and that interferences arising from the flagellar core are negligible. The number of helices in the sheath structure can be calculated (12). Previous determinations indicated two helices (15, 17), whereas our data suggest three. This discrepancy may be due to the different

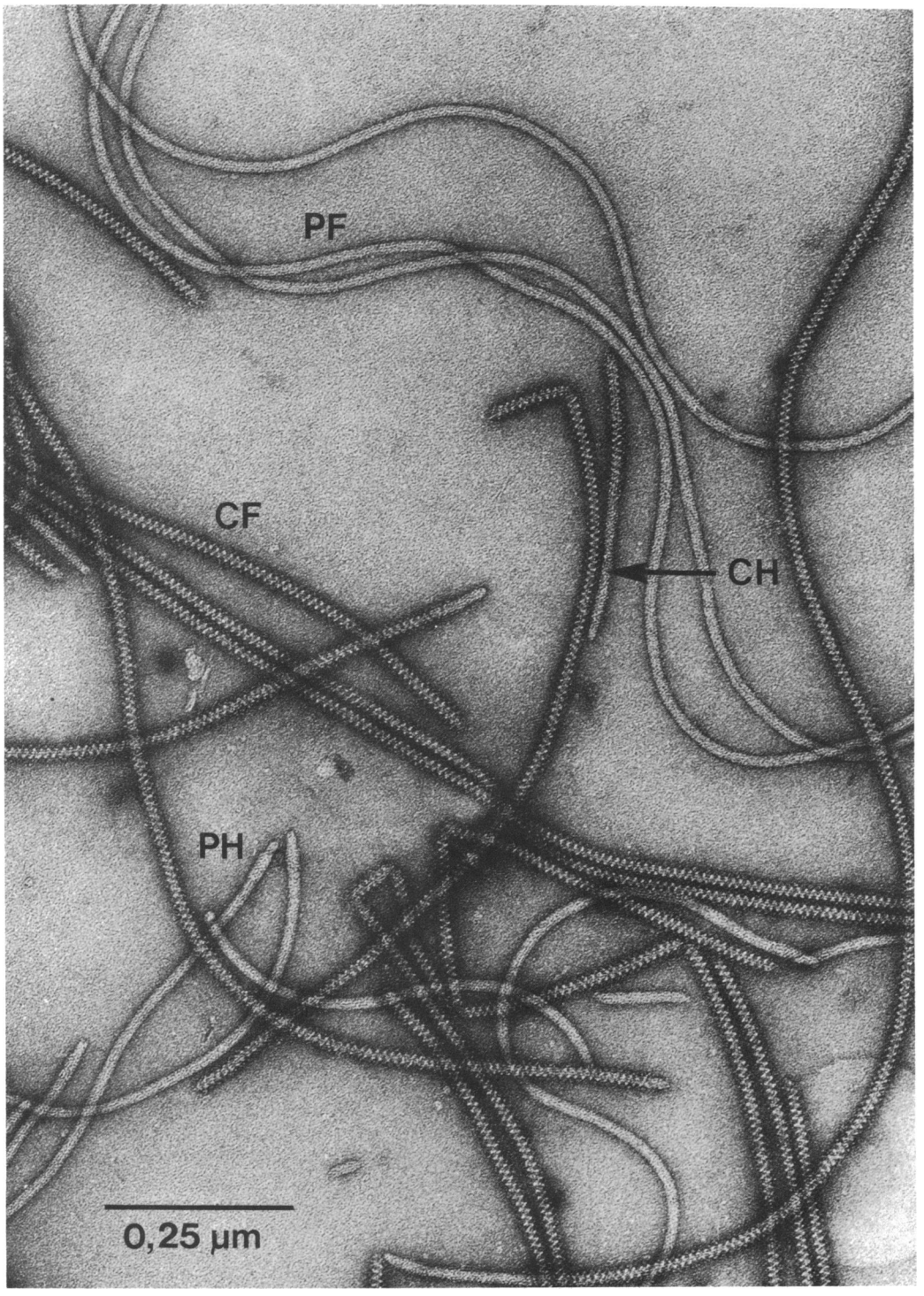

FIG. 1. *Isolated plain (PF) and complex (CF) flagella of P. rhodos 9-6, some with their hooks (PH and CH, respectively) attached. Negative staining with uranyl acetate.*

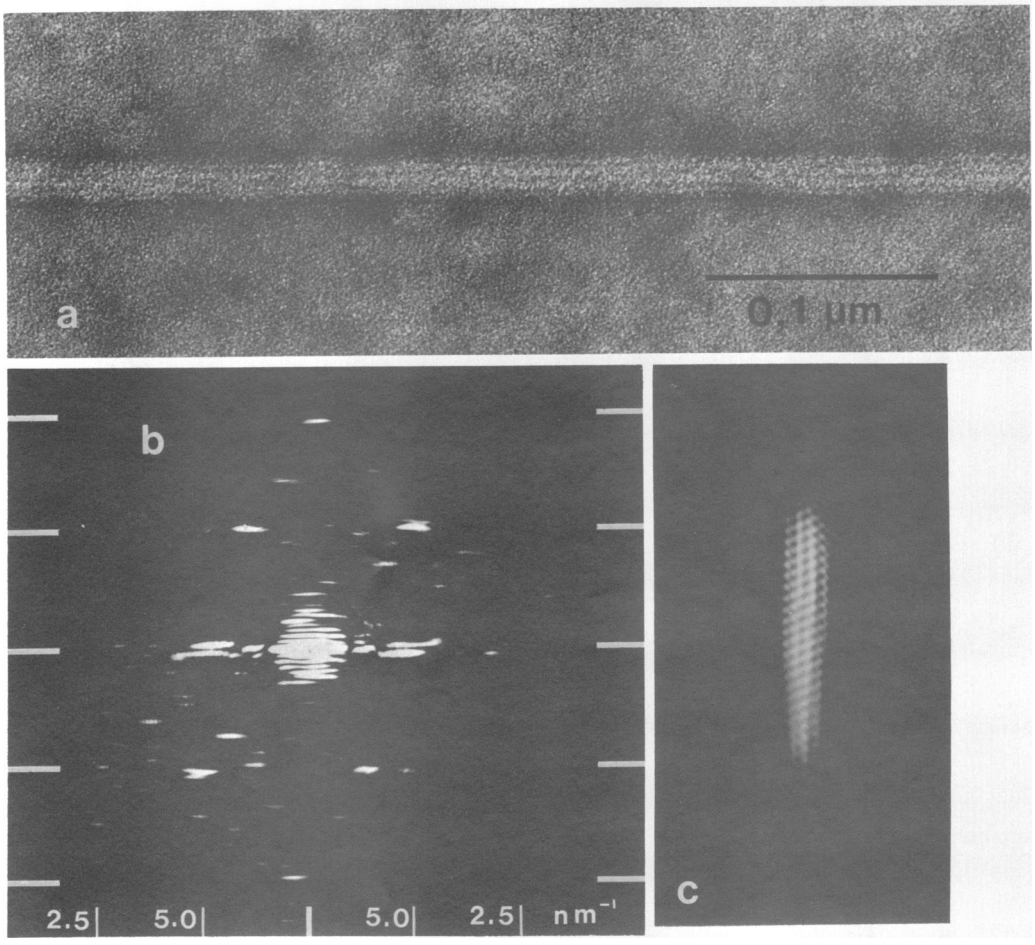

FIG. 2. (*a*) *Straight portion of a single plain flagellum showing four to five near-axial lines. The measured flagellar width of 21 nm indicates strong flattening of the particle. Negative staining with uranyl acetate.* (*b*) *Optical diffraction pattern of 2a. Layer lines at 4.5 nm*$^{-1}$ *spacing are shown for the principal maxima; reciprocal distances are indicated.* (*c*) *One-sided filtered image obtained from 2b.*

techniques employed for contrasting flagellar specimen and to uncertainties in determining the exact diameter of the flagellum. To decide whether the sheath structure is formed by two helical chains or three, consider the "zig-zag" pattern of complex flagella (Fig. 4). The apices formed by the superimposed helices alternate in position. Hence, the imaginary flagellar axis is a glide-reflection line found when there is an odd number of helices (18, 19). For an even number of helices, mirror-reflection symmetry would be expected. From this we have concluded that the sheath structure consists of three helical ribbons.

Electron micrographs of negatively stained complex flagella give little information on the internal core, because most of its structure is concealed by the helical sheath. Attempts to expose the core structure both by physical and chemical means were futile until it was found that treatment with 6 M urea at 25 C allowed a controlled decomposition of complex flagella. A portion of a urea-treated complex filament showing different stages of degradation is seen in Fig. 5. In one region (arrowed) an internal core of about 15-nm diameter is revealed. In adjacent regions, disintegration of the sheath structure has commenced. The section below the arrowed portion is of interest because it shows the extreme edges of the helical sheath which are normally covered by stain (see model in Fig. 4). It is possible to follow the curve of one or two helical ribbons for at least one period, confirming the presence of three helices in the

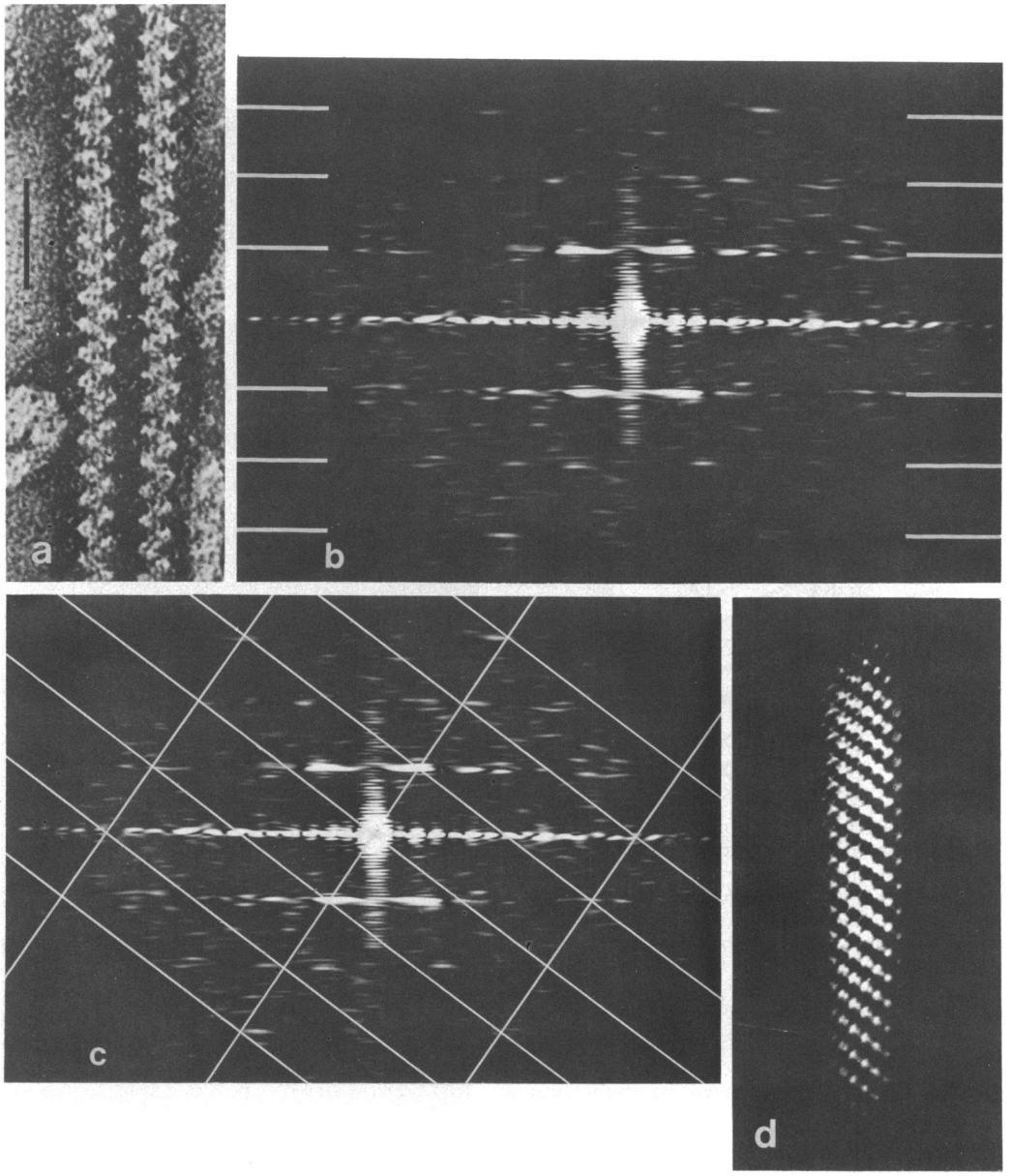

FIG. 3. *(a) Portion of two complex flagella showing the prominent "zig-zag" pattern of the helical sheath and several longitudinal lines thought to originate from the internal core structure. Negative staining with uranyl acetate. Bar marks 0.05 μm. (b) Optical diffraction pattern of one complex filament of 3a. Layer lines at 9.4 nm^{-1} spacing are indicated, corresponding to the distance of neighboring ribbons in the sheath structure (1 cm = 10.3 nm^{-1}). (c) Optical diffraction pattern as in 3b with the one-sided reciprocal lattice (of the helical sheath structure) superimposed. (d) One-sided filtered image of the helical sheath obtained from 3b by employing only maxima located on the reciprocal lattice.*

sheath structure. In a similarly treated sample (Fig. 6), an apparently intact complex filament is seen next to a naked core devoid of the helical sheath. The width of the core is about 13 nm. Along its entire length a stain-filled central tube of approximately 2.5-nm diameter can be discerned, a feature rarely seen under normal conditions (22). The partially decomposed hook

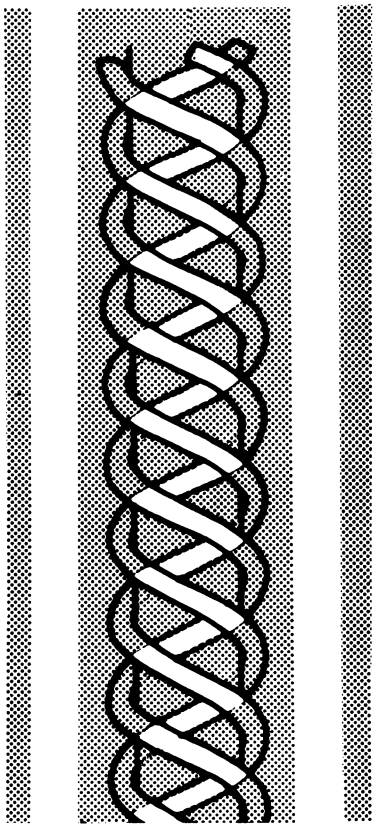

FIG. 4. *Model of a complex flagellar filament, illustrating the approximate stain distribution around a negatively stained particle by shading. The well-contrasted central region shows the superposition pattern of helical bands from "up" and "below" resulting in the characteristic "zig-zag." Note the glide-reflection symmetry of the overlapping regions ("apices") with respect to the flagellar axis indicating an odd number of helices. The model shows the actual number of three helical ribbons (see text).*

seen at one end of the core will be analyzed in a subsequent report (Raska, Mayer, and Schmitt, in preparation). Flat aggregates always found in urea-treated samples of complex flagella were identified as degradation products of the decomposed sheath structure. In contrast to the intact filament, which exhibits the typical flagellar curvature (2, 16), the overall shape of the naked core appears "soft." This could be either due to a general weakening of the core structure by urea or to the lack of the helical sheath as an essential requirement for the rigidity and overall shape of complex filaments.

Extended treatment with 6 M urea (longer than 20 min) frequently led to disintegration of the core into fibers coiled around each other (Fig. 7); under these conditions, flagellar hooks remained almost unaffected. If these fibers were

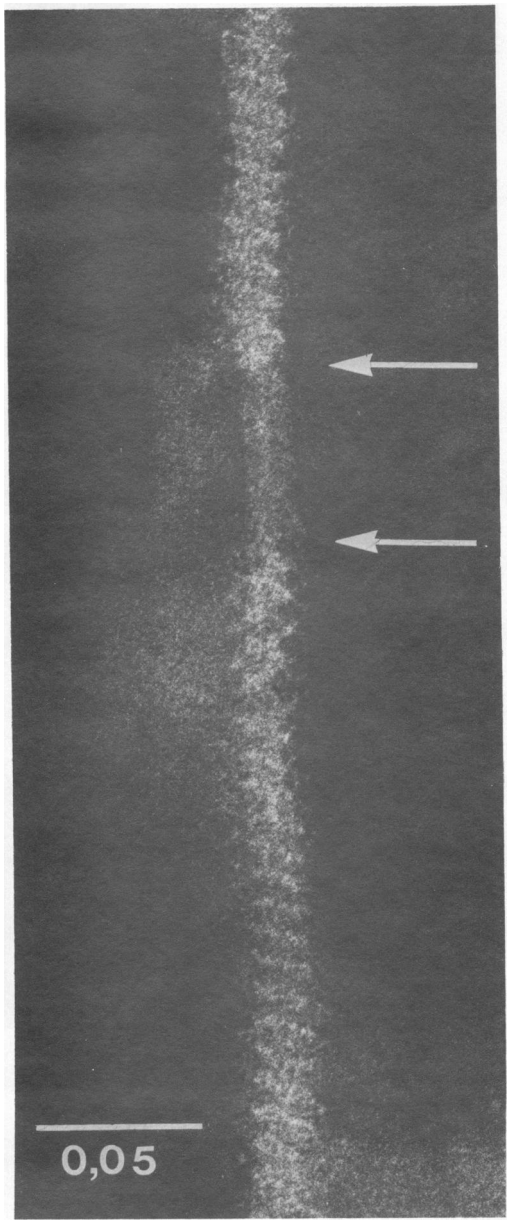

FIG. 5. *Portion of complex filament treated with 6 M urea. The arrowed region shows the exposed internal core; in the adjacent regions a progressive decomposition of the helical sheath is discernible. Extreme flattening of the particle is indicated by an increase of the flagellar width up to 50%. The extreme edges of the helical sheath can be viewed in one section (below arrows). Negative staining with potassium phosphotungstate. Dimension of mark in μm.*

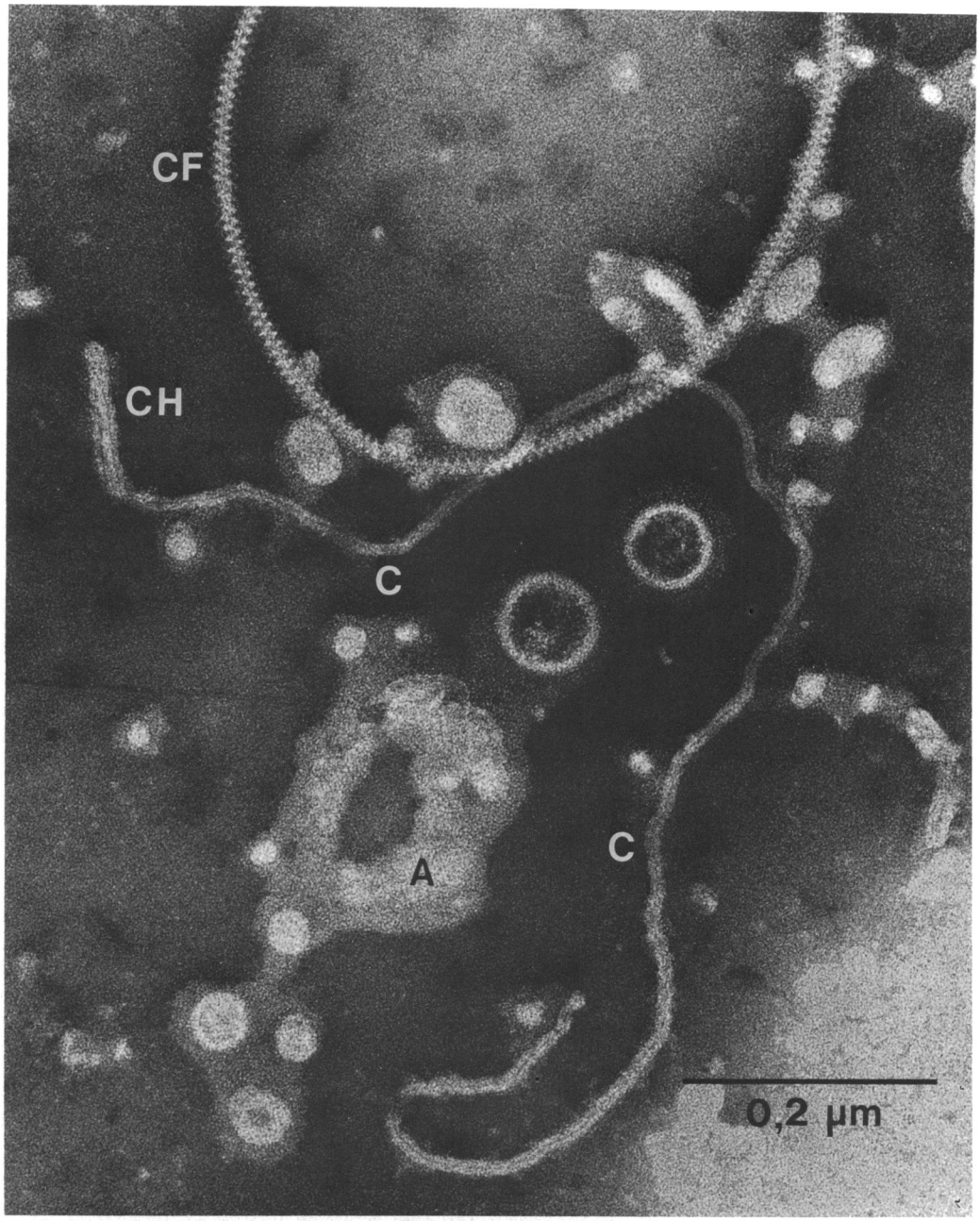

FIG. 6. *Complex flagella after treatment with 6 M urea. Portion of an intact filament (CF) and a naked core (C) with a partially disintegrated hook (CH) at one end. The overall structure of the core appears "soft," probably owing to the lack of the helical sheath; a central tube of about 2.5 nm width is discernible. Remnants of the decomposed sheath structure appear as flat aggregates (A). Negative staining with potassium phosphotungstate.*

formed by flagellin molecules normally arranged in longitudinal rows, a determination of their number (per flagellum) would allow an estimate of large-scale helices forming the core in the intact filament. Counting of fibers in regions where they appear well dispersed leads to values of 8 to 10 per bunch.

Finally, rare cases of apparently well-

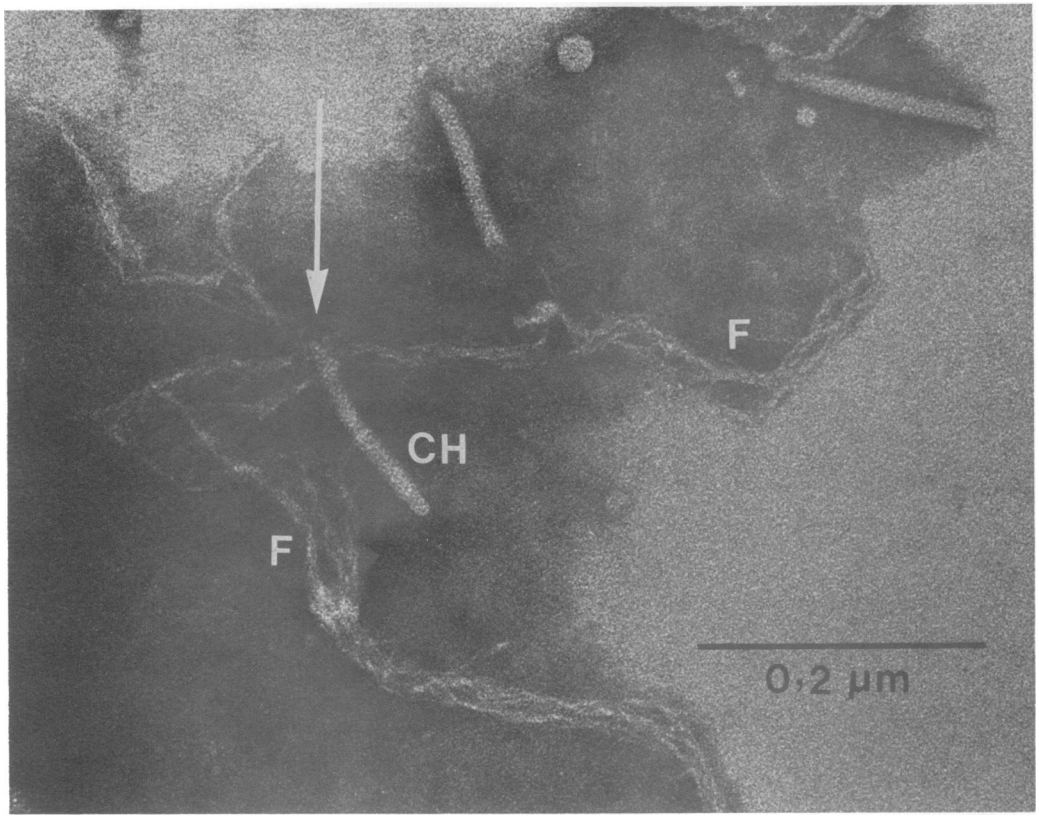

FIG. 7. *Complex flagella after protracted treatment with 6 M urea. Disintegration of internal cores into coiled bundles of eight to ten fibers (F) probably corresponding to rows of subunits originally arranged in large-scale helices. Arrow marks apparent origin of one bundle at a flagellar hook (CH), which under these conditions is not visibly decomposed. Negative staining with potassium phosphotungstate.*

preserved core structures were obtained after removal of the helical sheaths by urea treatment (Fig. 8a). The core lying across an aggregate of intact hooks has a width of 13 nm. Wedge-shaped incisions at one end of the core can be discerned in two places (arrowed), suggesting a polar arrangement of monomers in the cylindrical structure. This is a feature also found in common flagella (3, 19). The core shown in the inset of Fig. 8a has the best-preserved substructure. The diffractogram (Fig. 8b) taken of the marked region shows no reflections on layer lines of 9.4 nm^{-1} spacing (see Fig. 3b), indicating that the helical sheath has been completely removed. Prominent maxima on layer lines of 4.0 nm^{-1} spacing and near-equatorial reflections of 3.6 nm^{-1} spacing can be discerned. The meridional distribution of maxima asymmetric, indicating a mostly one-sided staining of the original particle (Fig. 8a). Moreover, subsidiary maxima are present in the diffractogram (Fig. 8b), suggesting that the cylindrical shape of the core is largely preserved (18). By assuming an outer diffracting radius of 6.5 nm (measured particle width: 13 nm), a lateral spacing of 4.4 nm of subunits can be calculated from the equatorial reflections (4). Hence, the number of longitudinal rows of subunits in a cylinder of 13-nm diameter ranges between 9 and 10, a value in agreement with the number of thin fibers seen in Fig. 7. A reciprocal lattice which accounts for the principal maxima has been superimposed on the diffractogram (Fig. 8b). The filtered and recombined image of the core is shown in Fig. 8c. Its surface lattice consists of globular subunits arranged in small-scale helices of pitch angle 31° and large-scale helices deviating approximately 2° from the cylinder axis.

Gel electrophoretic determination of flagellar composition. SDS gel electrophoresis (20) of mixed, plain and complex flagella isolated from *P. rhodos* 9-6 yields three protein bands which correspond to three subunit spe-

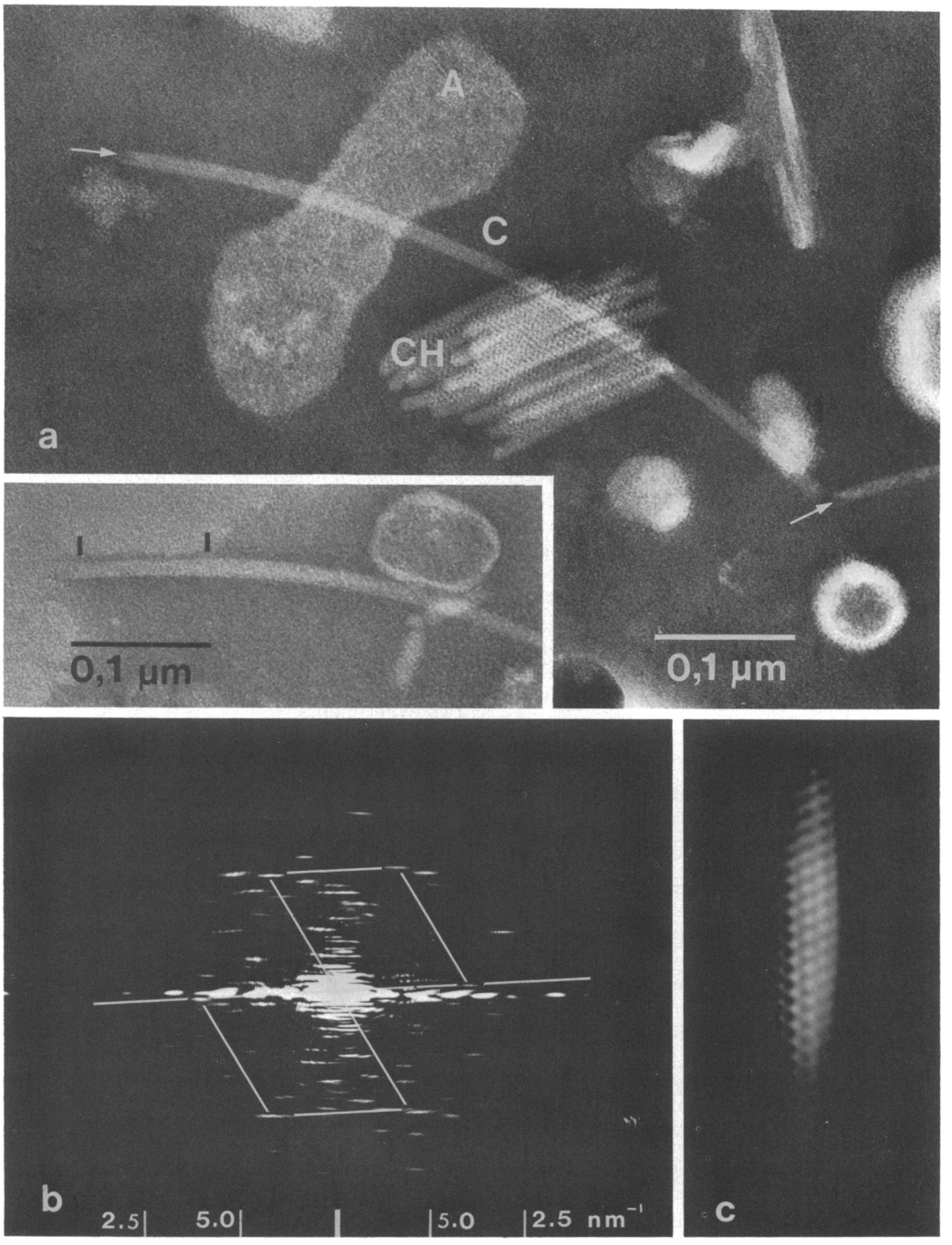

FIG. 8. *(a) Complex flagella after treatment with 6 M urea. Regular aggregate of non-decomposed flagellar hooks (CH), flat aggregates (A) of the decomposed sheath structure and well preserved internal cores (C) after complete removal of helical sheaths. Wedge-shaped incisions at one end (arrows) indicate the polar arrangement of subunits in the core; its globular substructure is discernible in the particle shown on the inset: Negative staining with potassium phosphotungstate. (b) Optical diffraction pattern of internal core (marked region in 8a). The one-sided reciprocal lattice shown accounts for the principal maxima on layer lines of 4.0 nm^{-1} spacing and for the near-equatorial reflections of 3.6 nm^{-1} spacing. (c) One-sided filtered image of the internal core obtained from 8b by employing reflections located on the reciprocal lattice.*

cies of different size (Fig. 9a). By comparison with homogeneous material isolated from mutant strains B9 (complex flagella) and D8 (plain flagella), respectively, the two slow-moving bands could be assigned to complex flagella and the fast-moving band to plain flagella. Subunit molecular weights were estimated by reference to standard proteins (Fig. 10). Molecular weights of 55,000 (major band) and 43,000 (minor band) are obtained for the two proteins of complex flagella and 37,000 for the monomer of plain flagella.

Gel electrophoresis in the presence of SDS is known to separate proteins according to their size and, hence, does not distinguish between polypeptide chains of equal molecular weight but different composition (5). In a different system which employs 8 M urea at pH 4.5 (25), electrophoretic mobilities are determined by the intrinsic molecular charges of the proteins in addition to their size. Under these conditions, complex flagella again were separated into a major and a minor subunit band. In contrast, the single protein band of plain flagella found in SDS gels splits into two bands of about equal intensity (Fig. 9b), indicating the presence of two slightly different monomers in these flagella. Whereas the subunit size of plain flagella appears normal (2, 8), the occurrence of two

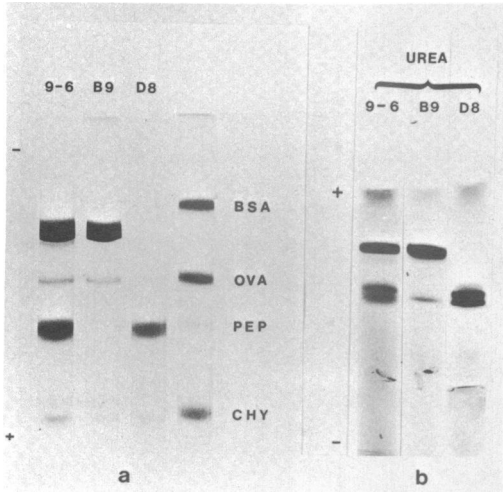

FIG. 9. *(a) SDS gel electrophoresis in 10% acrylamide. Subunit pattern of flagella isolated from strains 9-6 (plain and complex flagella), B9 (complex flagella), and D8 (plain flagella), respectively, compared to standard proteins (BSA, bovine serum albumin; OVA, ovalbumin S; PEP, pepsin; CHY, chymotrypsinogen). (b) Discontinuous gel electrophoresis in 10% acrylamide containing 8 M urea at pH 4.5 of flagellar proteins from strains 9-6, B9, and D8, respectively.*

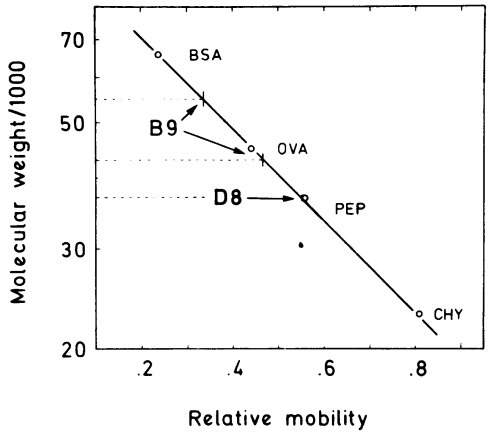

FIG. 10. *Semi-logarithmic plot of reference molecular weights versus relative electrophoretic mobilities (28) obtained from Fig. 9a for determining the molecular weights of flagellar proteins. Abbreviations as in Fig. 9.*

proteins of unusual molecular weight in complex flagella is a novel feature. Initially, it appeared obvious to assign these two protein species to the core (55,000) and the sheath structure (43,000), respectively. This assignment, however, was invalidated by the following two experiments.

(i) Densitometric scanning of SDS gels of independently isolated complex flagella revealed varying ratios of the two protein bands. In four experiments, the ratio of 55,000 to 43,000 molecular weight proteins differed between 6:1 and 11:1. Assuming a complete dissociation into subunits before gel electrophoresis, constant proportions of sheath and core subunits should be expected. The observed variation is, therefore, indicative of a separate origin of the two protein species.

(ii) Stepwise degradation of complex flagella by urea made a direct assignment of the two proteins possible. The incubation mixture containing isolated complex flagella and 6 M urea was sampled at intervals (see Materials and Methods). The kinetics of degradation followed by SDS gel electrophoresis over a 30-min period showed a rapid intensity decrease and the final disappearance of the 55,000 molecular weight protein band (Fig. 11). The 43,000 molecular weight band showed a slight decrease, but did not disappear. Parallel electron microscopy indicated a progressive decomposition of complex filaments and their final disintegration after 20 to 30 min. Flagellar hooks sometimes arranged in piles (Fig. 8a) were the only intact structures discernible at this time. This indicates that the

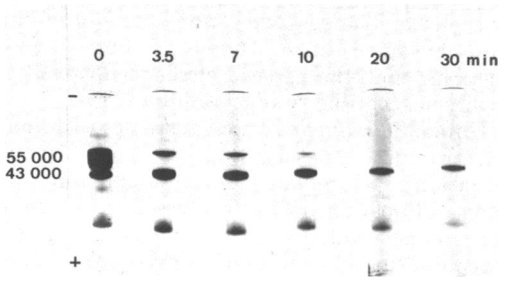

FIG. 11. *Decomposition kinetics of complex flagella by 6 M urea at 25 C followed by SDS gel electrophoresis in 7.5% acrylamide. Gels are marked at minute of sampling; the protein bands are indexed by molecular weights.*

complex filament, i.e., core and sheath, is composed of the 55,000 molecular weight protein and the 43,000 molecular weight protein represents a (major) structural component of the hook.

The sensitivity of complex filaments to a number of specific enzymes such as Pronase, trypsin, chymotrypsin, hyaluronidase, glucuronidase, and lipase was tested to prove its protein nature. Examination by electron microscopy and SDS gel electrophoresis indicated that only the proteolytic enzymes were capable of decomposing both the helical sheath and the core. None of the other enzymes had any effect on the structural integrity of the complex filament. Appreciable staining of the 55,000 molecular weight band occurred with Coomassie brilliant blue, which is known to be specific for proteins (6). Moreover, weak staining of this band by Alcian blue (27) could be observed, indicating a small carbohydrate moiety.

DISCUSSION

The results presented here indicate gross differences between the plain and complex flagella of *P. rhodos* 9-6. The diffraction pattern of a plain flagellar filament (Fig. 2) agrees essentially with the helical subunit arrangement proposed by Lowy and Spencer (16) for common bacterial flagella. The finding of two 37,000 molecular weight isoprotein molecules in plain flagella probably contributing to the same filament can be reconciled with the demonstration of two flagellin components in *B. pumilis* flagella by Oiler, Kocka, Smith, and Koffler (Bacteriol. Proc., p. 27, 1971). It remains to be shown whether the presence of two slightly different protomers in plain flagella pertains to their function in propagating helical waves (2, 9). The complex flagellum consists of a cylindrical core surrounded by a sheath consisting of three helical ribbons (Fig. 4). These are spaced at intervals—the axial latitude of chains and gaps appears to be equal. This close-fitting helical band structure is unusual and differs greatly from known flagellar sheaths, which are closed tubular structures contiguous with the cell wall (16, 23) and easily separable from their filaments (24). The complex sheath is intimately connected with the internal core. This became obvious as a result of difficulties encountered in attempting to remove the sheath without damaging the core structure. Furthermore, breakage of the complex flagellum never showed intact core structure protruding, as might be expected if the sheath and the core were less intimately associated. Exposing the core by a stepwise decomposition of the sheath with urea revealed a cylindrical filament of 13-nm diameter. Polarity of this structure is indicated by "chevrons" at one end (Fig. 8a), a feature also found in common flagella (3, 19). Extended urea treatment frequently led to disintegration of the core into bundles of 8 to 10 fibers (Fig. 7). These fibers are thought to arise by specific aggregation of subunits arranged in large-scale helices (16), indicating the direction of strain and their possible function as lines of contraction in the flagellar filament (4, 9). Similar observations were reported for acid-alcohol-treated *B. pumilis* flagella (1). A diffraction analysis of the complex flagellar core (Fig. 8b, c) suggests an arrangement of subunits in small-scale and large-scale helices similar but not identical to the substructure of plain flagella.

Differences in the fine structure of plain and complex flagella are parallel to distinctive physical and chemical properties, which demonstrate that they are entirely different flagellar species. In contrast to flexible plain flagella, complex filaments are fragile. They also exhibit greater thermostability than plain flagella. The subunit size of the two filaments is quite distinctive. The 37,000 molecular weight monomers of plain flagella are in contrast to a 55,000 molecular weight protein contained in the complex type. The molecular weight of this latter flagellin is unusually high and, to our knowledge, unique among the subunits of bacterial flagella (8, 23). Current research is directed at a large-scale purification of the 55,000 molecular weight protein to elucidate its shape and composition and to test our concept of the complex flagellar structure by reconstitution experiments.

By virtue of their unusual properties, the complex flagella of *P. rhodos* 9-6 may be consid-

ered unique among bacterial flagella. The tight connection of helical sheath and internal core and their composition of one protein species suggest that they are also functionally related. As seen in Fig. 6, the core structure stripped of its helical sheath appears "soft" and incapable of transmitting helical waves, whereas the portion of the intact filament shown exhibits the typical curvature required for flagellar function (2, 16). We suggest that the sheath is a superfolded triple helix fixed onto the core structure thus securing the shape and rigidity of the complex flagellum. In this model the core acts in longitudinally propagating helical waves, whereas the sheath is responsible for the maintenance of the three-dimensional helix structure thought to be a prerequisite for the passive transmission of mechanical energy from the cell membrane into the surrounding liquid (9).

The observation of mutant cells which carry one of the two types of flagellum shows that both flagellar species are capable of conferring motility to the cell. Cells with complex flagella exhibit an unusual spinning motion. A rapid spinning of cells has been described similarly for a mutant of *Escherichia coli* (21), which produces "polyhooks" acting like short filaments 1 to 2 μm in length. Active complex flagella may rarely surpass 2 μm in length because they tend to be easily broken and, therefore, are incapable of conferring normal translational motion. Alternatively, the hydrodynamic action of complex flagella may be different from that of plain flagella which are thought to act like an Archimedian screw (16). From our present data we cannot distinguish between these alternatives.

Electron and light microscope observations of wild-type *P. rhodos* revealed one polar or subpolar flagellum per cell (7, 17). By examining the motility of wild-type cells, we were able to distinguish between individuals with translational and those with spinning motion. This led us to conclude that plain and complex flagella may not be produced simultaneously but rather each species by a different cell. Such intraclonal variation in a genetically homogeneous strain has been termed "phase variation," a phenomenon well-studied in strains of *Salmonella*, which produce two antigenically distinct flagella (8). Diphasic strains may become stabilized in one or the other phase. This is controlled by a phase-specific regulatory gene determining which set of flagellar genes is switched on. The synthesis of plain and complex flagella by *P. rhodos* 9-6 can be interpreted in terms of a similar mechanism working at a high rate of variation. In this model, monophasic strains arise from inactivating mutations in the regulatory gene fixing flagellar synthesis in the respective phase. The ease with which such mutants were obtained in *P. rhodos* (5 out of 200) suggests that the genetic element involved is highly susceptible to mutation by NTG.

Unlike *Salmonella*, which possesses two similar structural genes for flagellin synthesis, the situation in *P. rhodos* cannot be explained by gene duplication owing to gross differences in the composition of the two flagellar species. Possibly, the acquisition of an extra set of genes for flagellar synthesis may reflect a distant event in the history of this bacterium. The observed differences in motion generated by plain and complex flagella, respectively, may confer a selective advantage to strains which harbor both flagellar species. Cells of *P. rhodos* are capable of forming stable aggregates ("stars") for conjugation (7), an accomplishment which may be favored by a specialized type of motion in the natural environment.

ACKNOWLEDGMENTS

We thank Wolfram Heumann for the gift of *P. rhodos* 9-6 and for his steady interest in this work. We are indebted to Edward Kellenberger for stimulating discussions and to Allan Vivian for his helpful criticism in reviewing the manuscript. The excellent technical assistance of Ingeborg Bamberger, Beatrix Görg, Angelika Poy, José Roempler, and Claus Edelbluth is gratefully acknowledged.

This work was supported by grants from the Deutsche Forschungsgemeinschaft and the Stiftung Volkswagenwerk. Joint research at the University of Geneva was facilitated by an EMBO long-term fellowship to I.R. and EMBO short-term fellowships to F.M. and R.S.

LITERATURE CITED

1. Abram, D., J. R. Mitchen, H. Koffler, and A. E. Vatter. 1970. Differentiation within the bacterial flagellum and isolation of the proximal hook. J. Bacteriol. **101**:250-261.
2. Asakura, S. 1970. Polymerization of flagellin and polymorphism of flagella. Advan. Biophys. (Japan) **1**:99-155.
3. Bode, W., J. Engel, and D. Winkelmair. 1972. A model of bacterial flagella based on small-angle X-ray scattering and hydrodynamic data which indicate an elongated shape of the flagellin protomer. Eur. J. Biochem. **26**:313-327.
4. Champness, J. N. 1971. X-ray and optical diffraction studies of bacterial flagella. J. Mol. Biol. **56**:295-310.
5. Dunker, A. K., and R. R. Rueckert. 1969. Observations on molecular weight determinations on polyacrylamide gel. J. Biol. Chem. **244**:5074-5080.
6. Fischbein, W. N. 1972. Quantitative densitometry of 1 to 50 μg protein in acrylamide gel slabs with Coomassie blue. Anal. Biochem. **46**:388-401.
7. Heumann, W. 1962. Die Methodik der Kreuzung sternbildender Bakterien. Biol. Zentralbl. **81**:341-354.
8. Iino, T. 1969. Genetics and chemistry of bacterial flagella. Bacteriol. Rev. **33**:454-475.
9. Klug, A. 1967. The design of self-assembling systems of equal units. Symp. Int. Soc. Cell Biol. **6**:1-18.
10. Klug, A., F. H. C. Crick, and H. W. Wyckoff. 1958. Diffraction by helical structures. Acta Crystallogr. **11**:199-213.

11. Klug, A., and D. J. De Rosier. 1966. Optical filtering of electron micrographs: reconstruction of one-sided images. Nature (London) **212**:29-32.
12. Labaw, L. W., and V. M. Moseley. 1954. Periodic structure in the flagella and cell walls of a bacterium. Biochim. Biophys. Acta **15**:325-331.
13. Lowry, O. H., N. J. Rosebrough, A. L. Farr, and R. J. Randall. 1951. Protein measurement with the Folin phenol reagent. J. Biol. Chem. **193**:265-275.
14. Lowy, J. 1965. Structure of the proximal ends of bacterial flagella. J. Mol. Biol. **14**:297-299.
15. Lowy, J., and J. Hanson. 1965. Electron microscope studies of bacterial flagella. J. Mol. Biol. **11**:293-313.
16. Lowy, J., and M. Spencer. 1968. Structure and function of bacterial flagella. Symp. Soc. Exp. Biol. **22**:215-236.
17. Marx, R., and W. Heumann. 1962. Über Geißelfeinstrukturen und Fimbrien bei zwei *Pseudomonas*-Stämmen. Arch. Mikrobiol. **43**:245-254.
18. Moody, M. F. 1967. Structure of the sheath of bacteriophage T4. I. Structure of the contracted sheath and polysheath. J. Mol. Biol. **25**:167-200.
19. O'Brien, E. J., and P. M. Bennett. 1972. Structure of straight flagella from a mutant *Salmonella*. J. Mol. Biol. **70**:133-152.
20. Shapiro, A. L., E. Vinuela, and J. V. Maizel, Jr. 1967. Molecular weight estimation of polypeptide chains by electrophoresis in SDS-polyacrylamide gels. Biochem. Biophys. Res. Commun. **28**:815-820.
21. Silverman, M. R., and M. I. Simon. 1972. Flagellar assembly mutants in *Escherichia coli*. J. Bacteriol. **112**:986-993.
22. Sleytr, U. B., and A. M. Glauert. 1973. Evidence for an empty core in a bacterial flagellum. Nature (London) **241**:542-543.
23. Smith, R. W., and H. Koffler. 1971. Bacterial flagella. Advan. Microbiol. Physiol. **6**:219-339.
24. Tauschel, H. D. 1970. Der Geisselapparat von *Rhodopseudomonas palustris*. IV. Isolierung der Geissel und ihrer Komponenten. Arch. Mikrobiol. **74**:193-206.
25. Traut, R. R. 1966. Acrylamide gel electrophoresis of radioactive ribosomal protein. J. Mol. Biol. **21**:571-576.
26. Valentine, R. C., B. M. Shapiro, and E. R. Stadtman. 1968. Regulation of glutamine synthetase. XII. Electron microscopy of the enzyme from *Escherichia coli*. Biochemistry **7**:2143-2152.
27. Wardi, A. H., and G. A. Michos. 1972. Alcian blue staining of glycoproteins in acrylamide disc electrophoresis. Anal. Biochem. **49**:607-609.
28. Weber, K., and M. Osborn. 1969. The reliability of molecular weight determinations by dodecylsulfate-polyacrylamide gel electrophoresis. J. Biol. Chem. **244**:4406-4412.
29. Yanagida, M., E. Boy de la Tour, C. Alff-Steinberger, and E. Kellenberger. 1970. Studies on the morphopoesis of the head of bacteriophage T-even. J. Mol. Biol. **50**:35-38.